2018 15th International Conference on
Control, Automation, Robotics and Vision (ICARCV)
Singapore, November 18-21, 2018

Model-free Approach for Sensor Network Localization with Noisy Distance Measurement

Xu Fang, Chen Wang, Thien-Minh Nguyen and Lihua Xie *Fellow, IEEE*

***Abstract*— A model-free localization method with noisy distance measurement is proposed for estimating a moving robot in 3D space. Considering that the traditional filter-based sensor network localization algorithms can not provide acceptable estimation accuracy in altitude in 3D space, the proposed method utilizes not only current measurements but also previous measurements to localize a robot. This character adds more constraints to localization to avoid local minimum. In addition, different from the traditional filter-based localization methods which need kinetic model for localization, our proposed method is model-free and converts the localization problem to graph optimization problem. The advantage is that we avoid the possible estimation error caused by inaccurate or simplified kinetic model. Considering that the communication limitation in application makes many graph optimization theories such as distributed localization theory and trilateration difficult to be realized, our method proposes to add constrained equation between adjacent positions to solve this problem. Experiments under a variety of scenarios verify the stability of this method and show that the algorithm achieves better localization accuracy than filter-based methods.**

I. INTRODUCTION

Target localization has been extensively studied and is widely used in the robot-related applications. For outdoor localization, the widely used localization system is Global Positioning System (GPS). This technique can provide accurate estimation for robots in the line-of-sight environment. But GPS can not be used for indoor localization due to the non-line-of-sight blockage in indoor environment. For indoor localization, WiFi-based methods [5], [22] can estimate a robot with estimation accuracy about one meter which is unacceptable for applications such as formation and swarming. Vision-based localization methods [15], [2] can not be applied to robots with ultra-low power processor such as Raspberry Pi processor. Therefore, researchers try to use noisy distance measurement from ultra-wideband (UWB) sensor to estimate a moving robot in indoor environment.

Ultra-wideband is a radio-technology that can use a very low energy level for short-range, high-bandwidth communication over a large portion of the radio spectrum. The general problem in UWB-based localization is how to localize a moving robot using distance measurements from the known fixed UWB anchors. The existing results using UWB for localization can be found in [17], [14], [1], [12], [7]. For UWB-based localization, the robots [19] are able to locate themselves by using a set of fixed anchors, and an extended aerodynamic model for localization under the assumption of no wind. The specification of a time of flight-based ranging protocol [6] is proposed for localization without involving a localization server. Cooperative UWB localization tackling the trade-off between accuracy and delay is considered in [11], which derives lower bounds on UWB positioning accuracy. For localization-related applications, the localization is applied to swarms of robots in [21], which utilizes tessellated maps that associate probabilistic error models for localization. The capability of supporting multi-UAV formation is presented in [20]. But this localization system needs to be fused with other sensors to obtain altitude estimation.

The existing UWB-based localization methods in real applications are mainly filter-based methods such as Kalman filter, extended Kalman filtering (EKF), unscented Kalman filtering (UKF) and particle filtering [4], [10]. However, an obvious problem is that these methods heavily rely on an accurate kinetic model, which is hard to obtain due to the complex structure of robots. The EKF and UKF will also suffer from linearization for nonlinear dynamic models. The Kalman filter is only applicable to a linear kinetic model. So the accuracy of localization will be dramatically influenced, when the state equations are nonlinear.

The filter-based localization methods can not provide acceptable estimation accuracy in altitude in 3D space (estimation error is about 40 centimeters). Filter-based localization methods only utilize current measurement and a priori estimate for each estimation, but our approach utilizes not only current measurements but also previous measurements. This character adds more constraints to localization to avoid local minimum.

Also, our proposed algorithm is model-free and does not need kinetic model. The localization problem is converted to graph optimization problem. However, existing graph optimization theories [8], [3] can not be used for estimating a moving robot due to communication limitation. At each time instant, robot can only receive one measurement from one UWB anchor. This is the reason why distributed localization theories and trilateration can not be used for estimating moving robot because at each time instant they need to receive distance measurements from all fixed UWB anchors which is impossible in real application. We proposes to add constrained equation between adjacent positions to solve this problem. Our method achieves better estimation accuracy in 3D space than existing filter-based methods under the same conditions.

This paper is organized as follows: Section II provides

Xu Fang and Chen Wang are joint first authors.
The authors are with School of Electrical and Electronic Engineering, Nanyang Technological University, Singapore (e-mail: fa0001xu@e.ntu.edu.sg, wang.chen@zoho.com, e150040@e.ntu.edu.sg, elhxie@ntu.edu.sg).

978-1-5386-9582-1/18/$31.00 ©2018 IEEE

a summary of relevant mathematical preliminaries for localization. In section III, basic concepts about localization are presented. Section IV shows the problem formulation of our proposed method. Section V presents the optimization method used for solving the cost function. Section VI provides the details of experiments for localization. Section VII ends this paper with conclusions.

II. Preliminary

In this section, a summary of relevant mathematical concepts about 3D transformation are presented.

A. Manifold, Lie group and Lie algebra

Manifold is a topological space that locally resembles Euclidean space near each point. A group is an algebraic structure consisting of a set of elements equipped with an operation that combines any two elements to form a third element. The group SE(3) is Lie group [13] which is a smooth manifold. Considering the robot motion in 3D space, poses of robot can be regarded as transformation (such as SE(3) in 3D space). The element of SE(3) can be shown by:

$$\mathbf{P} = \begin{bmatrix} \mathbf{R}_r & \mathbf{t} \\ \mathbf{0} & 1 \end{bmatrix} \in \text{SE(3)}, \quad \mathbf{R}_r \in \text{SO(3)}, \quad \mathbf{t} \in \mathbb{R}^3, \tag{1}$$

where $\mathbf{P}$ is transformation, $\mathbf{R}_r$ is rotation matrix and $\mathbf{t}$ is translation vector. The elements in rotational group SO(3) are orthogonal matrices. The exponential map takes the Lie algebra $\mathfrak{so}(3)$ to rotation group SO(3) shown as following:

$$\begin{aligned} \omega &= (\omega_1, \omega_2, \omega_3)^T \in \mathbb{R}^3, \\ \omega_\times &= \begin{bmatrix} 0 & -\omega_3 & \omega_2 \\ \omega_3 & 0 & -\omega_1 \\ -\omega_2 & \omega_1 & 0 \end{bmatrix} \in \mathfrak{so}(3), \\ \mathbf{R}_r &= exp(\omega_\times) \in \text{SO(3)}, \end{aligned} \tag{2}$$

where $\omega_\times$ is skew symmetric matrices which belong to Lie algebra $\mathfrak{so}(3)$. The rotation matrix $\mathbf{R}_r$ can be mapped into vector space ω. Similarly, the relationship between Lie algebra $\mathfrak{se}(3)$ and Lie group SE(3) is shown by:

$$\begin{aligned} \epsilon &= (\omega, \mathbf{u})^T \in \mathbb{R}^6, \quad \omega, \mathbf{u} \in \mathbb{R}^3, \\ \epsilon_\times &= \begin{bmatrix} \omega_\times & \mathbf{u} \\ \mathbf{0} & 0 \end{bmatrix} \in \mathfrak{se}(3), \\ \mathbf{P} &= exp(\epsilon_\times) \in \text{SE(3)}. \end{aligned} \tag{3}$$

Then definition of $\mathbf{log}_{\text{SE(3)}}(\cdot)$ is designed by:

$$\mathbf{log}_{\text{SE(3)}}(\mathbf{P}) = \epsilon. \tag{4}$$

B. Operator for Lie-groups

The Lie group SE(3) is a kind of manifold, which consists of rotation matrix and translation vector. The translation vector $\mathbf{t}$ forms a Euclidean space but the rotation matrix $\mathbf{R}_r$ span over non-Euclidean space. So conventional optimization methods applied in Euclidean space can not solve optimization problem on Lie-Manifolds. One method is to map manifold into Euclidean space. From (3), we can know $\epsilon \in \mathbb{R}^6$ is the corresponding vector mapped from transformation $\mathbf{P}$ in 3D space. So group SE(3) can be mapped into Euclidean space.

For the two transformations $\mathbf{P}_1, \mathbf{P}_2 \in$ SE(3), corresponding vectors are $\epsilon_1, \epsilon_2 \in \mathbb{R}^6$. The transformation $\mathbf{M}$ moving $\mathbf{P}_1$ to $\mathbf{P}_2$ can be represented by $\mathbf{P}_2 = \mathbf{P}_1 \cdot \mathbf{M}$, and mathematical relation among ϵ_1, ϵ_2 and ϵ_M is expressed by:

$$\text{SE(3)}^{\epsilon_2} = \text{SE(3)}^{\epsilon_1} \cdot \text{SE(3)}^{\epsilon_M}. \tag{5}$$

This kind of mapping is not unique. We choose (5) in this paper.

III. Basic Concepts for Localization

Given two transformations $\mathbf{P}_1, \mathbf{P}_2 \in$ SE(3), their corresponding rotation matrices $\mathbf{R}_{r1}$, $\mathbf{R}_{r2}$ and translation vectors $\mathbf{t}_1 = (t_{1x}, t_{1y}, t_{1z})^T$, $\mathbf{t}_2 = (t_{2x}, t_{2y}, t_{2z})^T$, three kinds of measurement variables are given by:

1) Transformation measurement variable $\hat{\mathbf{z}}_k \in$ SE(3):

$$\hat{\mathbf{z}}_k = \mathbf{P}_1^{-1} \cdot \mathbf{P}_2 = \begin{bmatrix} \mathbf{R}_{r1} & \mathbf{t}_1 \\ \mathbf{0} & 1 \end{bmatrix}^{-1} \cdot \begin{bmatrix} \mathbf{R}_{r2} & \mathbf{t}_2 \\ \mathbf{0} & 1 \end{bmatrix}. \tag{6}$$

2) Translational measurement variable $\hat{\mathbf{z}}_k \in \mathbb{R}^3$:

$$\hat{\mathbf{z}}_k = \mathbf{t}_2 - \mathbf{t}_1, \tag{7}$$

.

Suppose that $\hat{\mathbf{y}}_k$ is predicted measurement, in 3-D space, three kinds of measurement functions are designed as following:

1) Transformation measurement function.

$$\hat{\mathbf{y}}_k = \mathbf{log}_{\text{SE(3)}}(\hat{\mathbf{z}}_k), \tag{8}$$

where $\hat{\mathbf{z}}_k \in$ SE(3).

2) Translational measurement function.

$$\hat{\mathbf{y}}_k = \hat{\mathbf{z}}_k, \quad \hat{\mathbf{z}}_k \in \mathbb{R}^3, \tag{9}$$

3) Distance measurement function.

$$\hat{y}_k = ||\hat{\mathbf{z}}_k||_2, \quad \hat{\mathbf{z}}_k \in \mathbb{R}^3. \tag{10}$$

Two kinds of measurement variables $\hat{\mathbf{z}}_k$ are mapped into Euclidean space by the above measurement functions.

A GPS-denied localization system for moving robot is proposed with a small number of anchors placed in fixed positions, and the robot is equipped with one UWB module. The localization algorithm uses measurements from UWB and IMU detailed below.

IV. Problem Formulation

The UWB module can use either one-way communication or two-way communication to receive a distance measurement. UWB modules can also send data to each other.

Our UWB ranging algorithm uses two-way TOA measurement to calculate the distance [17]. The distance measurement $d \in \mathbb{R}$ can be obtained from the synchronized TOA measurement T_{ra}:

$$d = (T_{ra} - \Delta T_{ra}) \cdot c + n_{ra}, \tag{11}$$

where ΔT_{ra} is the processing time delay, c is the speed of light, and n_{ra} is the measurement noise.

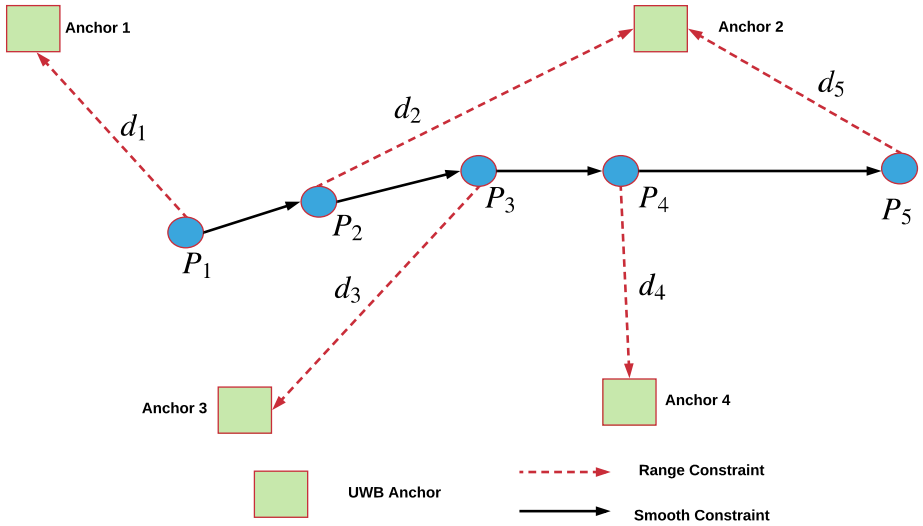

Fig. 1. Localization system used for constructing constrained equations are shown in this figure. The robot moves in 3-D space and four anchors are placed in fixed positions. The robot is equipped with UWB module. For example, The robot moves from P_1 to P_4 and gets four distance measurements (d_0 to d_3) from four fixed anchors.

The constrained equation between robot translation $\mathbf{t}_k$ and fixed anchor translation $\mathbf{t}_\mathbf{i}^\mathbf{anchor}(i = 1, 2, 3, 4)$ is designed as:

$$E_k^r = \rho(e_k^r w_k^r e_k^r), \tag{12a}$$

$$e_k^r = d_k - ||\mathbf{t}_k - \mathbf{t}_\mathbf{i}^\mathbf{anchor}||_2, \tag{12b}$$

where k is the time instant at which a measurement is acquired. i is the label of fixed anchor shown in Fig. 1. d_k is the measured distance between robot translation $\mathbf{t}_k$ and fixed anchor translation $\mathbf{t}_\mathbf{i}^\mathbf{uwb}$ at time instant k. where $\rho(\cdot)$ is the Pseudo-Huber loss function defined as $\rho(q) = \delta^2(\sqrt{1 + (q/\delta)^2} - 1)$. w_k^r is a penalty term given by:

$$w_k^r = \frac{\iota^2}{||\Omega_k^r||_2^2 + \iota^2}, \tag{13}$$

where ι is a free-parameter and $\Omega_k^r \in \mathbb{R}$ is the variance of the distance measurement d_k.

(12) only gives a constraint on a set of sparse points and fails to form a smooth trajectory. A constrained equation between adjacent transformations ($\mathbf{P}_k$ and $\mathbf{P}_{k-1}$) is needed to smooth the trajectory.

For adjacent transformations $\mathbf{P}_k$ and $\mathbf{P}_{k-1}$ (transformation is defined in (1)), the transformation constraint between $\mathbf{P}_k$ and $\mathbf{P}_{k-1}$ is designed as:

$$\mathbf{P}_{k-1}^{-1} \cdot \mathbf{P}_k = \begin{bmatrix} \mathbf{R}_{k-1}^{-1}\mathbf{R}_k & \mathbf{R}_{k-1}^{-1}(\mathbf{P}_k - \mathbf{P}_{k-1}) \cdot (0,0,0,1)^T \\ \mathbf{0} & 1 \end{bmatrix}. \tag{14}$$

The rotations $\mathbf{R}_k$ and $\mathbf{R}_{k-1}$ are obtained from IMU. The constrained equation between $\mathbf{P}_k$ and $\mathbf{P}_{k-1}$ is designed as:

$$E_k^p = \rho(\|\mathbf{e}_k^{pT}\mathbf{w}_k^p\mathbf{e}_k^p\|_2), \tag{15a}$$

$$\mathbf{e}_k^p = \mathbf{log}_{\mathrm{SE(3)}}(\mathbf{P}_{k-1}^{-1} \cdot \mathbf{P}_k), \tag{15b}$$

where $\mathbf{e}_k^p$ is a vector from (4) and matrix $\mathbf{w}_k^p$ is term penalty shown as:

$$\mathbf{w}_k^p = \begin{bmatrix} \mathbf{\Omega}_k^o & \mathbf{0} \\ \mathbf{0} & \mathbf{\Omega}_k^t \end{bmatrix}, \tag{16}$$

with $\mathbf{\Omega}_k^o \in \mathbb{R}^{3\times3}$ and $\mathbf{\Omega}_k^t \in \mathbb{R}^{3\times3}$ being the covariance matrices of orientation and translation. $\mathbf{\Omega}_k^t$ is a diagonal matrix with diagonal elements $\frac{9\iota^2}{||v_{max}\cdot\Delta T||_2^2+9\iota^2}$ if we can not obtain robot velocity.

The design of smooth edge is the key point for the success of estimating moving robot in 3D space, which is never used in UWB-based localization before. The existing methods use (12) and kinetic model for localization. The existing graph realization methods only use (12) for estimating fixed anchors, which can not be used for estimating moving robot. Our method is the combination of (12) and (15). A trajectory $\mathbf{P} = (\mathbf{P}_1, \mathbf{P}_2, \cdots, \mathbf{P}_k)$ can be obtained by the following cost function:

$$F_{rp}(\mathbf{P}_1, \mathbf{P}_2, \cdots, \mathbf{P}_k) = \sum_{i=1}^{k}(E_i^r + E_i^p), \tag{17a}$$

$$\mathbf{P}^* = (\mathbf{P}_1^*, \mathbf{P}_2^*, \cdots, \mathbf{P}_k^*) = \arg\min F_{rp}(\mathbf{P}_1, \mathbf{P}_2, \cdots, \mathbf{P}_k). \tag{17b}$$

where $\mathbf{P}^* = (\mathbf{P}_1^*, \mathbf{P}_2^*, \cdots, \mathbf{P}_k^*)$ is estimated trajectory. $\mathbf{P}_i^*(i = 1, 2, \cdots, k)$ represents estimated robot transformation at time instant i. $\mathbf{P}_1^*$ is estimated initial transformation of the robot. The estimated transformations $\mathbf{P}^* = (\mathbf{P}_1^*, \mathbf{P}_2^*, \cdots, \mathbf{P}_k^*)$ include the estimated translations $\mathbf{t}^* = (\mathbf{t}_1^*, \mathbf{t}_2^*, \cdots, \mathbf{t}_k^*)$ and estimated rotations $\mathbf{R}^* = (\mathbf{R}_1^*, \mathbf{R}_2^*, \cdots, \mathbf{R}_k^*)$.

V. Graph Optimization

For the transformations $\mathbf{P} = (\mathbf{P}_1, \mathbf{P}_2, \cdots, \mathbf{P}_k)$, all the translation vectors $\mathbf{t}$ form an Euclidean space but the rotation

matrices $\mathbf{R}$ span over a non-Euclidean space. Therefore, the cost function (17) is optimized on Lie-manifold.

We can know each transformation $\mathbf{P}_k$ corresponds a vector ϵ_k over a non-Euclidean space from (15). To find an optimal solution in a non-Euclidean space, an idea is that we map Manifold into Euclidean space by (4) [16]. The cost function (15) becomes:

$$F_{rp}(\epsilon_1, \epsilon_2, \cdots, \epsilon_k) = \sum_{i=1}^{k} (E_i^r + E_i^p), \tag{18a}$$

$$\epsilon^* = (\epsilon_1^*, \epsilon_2^*, \cdots, \epsilon_k^*) = \arg\min F_{rp}(\epsilon_1, \epsilon_2, \cdots, \epsilon_k). \tag{18b}$$

The e_k^r and $\mathbf{e}_k^p$ in (12) and (15) can be defined as:

$$\mathbf{e}_k(\widetilde{\epsilon}_k + \Delta\epsilon_k) \simeq \mathbf{e}_k(\widetilde{\epsilon}_k) + \mathbf{J}_k \Delta\epsilon_k. \tag{19}$$

where $\widetilde{\epsilon}_k$ is the initial guess and $\Delta\epsilon_k$ is the increment.

The jacobian matrix $\mathbf{J}_k$ can be calculated by:

$$\mathbf{J}_k = \left. \frac{\partial \mathbf{e}_k(\widetilde{\epsilon}_k + \Delta\epsilon_k)}{\partial \Delta\epsilon_k} \right|_{\Delta\epsilon_k = 0}. \tag{20}$$

For cost function (18), the optimized increment $\Delta\epsilon = (\Delta\epsilon_1, \Delta\epsilon_2, \cdots, \Delta\epsilon_k)$ can be acquired by Levenberg-Marquardt method [18]. Then the optimized solution $\epsilon^* = (\epsilon_1^*, \epsilon_2^*, \cdots, \epsilon_k^*)$ to cost function (18) is obtained by :

$$\epsilon^* = \widetilde{\epsilon} + \Delta\epsilon, \quad \widetilde{\epsilon} = \epsilon^*. \tag{21}$$

The optimization process continues until the maximum iteration number is reached. After obtaining the optimal solution $\epsilon^* = (\epsilon_1^*, \epsilon_2^*, \cdots, \epsilon_k^*)$, the estimated trajectory $\mathbf{P}^* = (\mathbf{P}_1^*, \mathbf{P}_2^*, \cdots, \mathbf{P}_k^*)$ can be obtained by (4).

A. Noise distribution

Gaussian distribution over transformations in Lie group G has a mean transformation $\mu \in G$ and covariance matrix $\sum \in \mathbb{R}^{k \times k}$[9]. For a sample noise $\tilde{x}$ which is from the Gaussian distribution in Lie space $(\mu, \sum)$ with mean μ satisfying

$$\tilde{x} = exp(\epsilon_\times) \cdot \mu, \tag{22}$$

where $\epsilon_\times$ is from Gaussian distribution $\epsilon_\times \in N(0, \sum)$. For any $y \in G$, the transformed noise distribution $y \cdot \tilde{x}$ is

$$\begin{aligned} &y \cdot \tilde{x} = y \cdot exp(\epsilon_\times) \cdot \mu = exp(Adj_y \cdot \epsilon_\times) \cdot y \cdot \mu, \\ &\epsilon_\times \in se(3), exp(\epsilon_\times) = \begin{bmatrix} \mathbf{R} & \mathbf{t} \\ \mathbf{0} & 1 \end{bmatrix} \in \text{SE(3)}, \\ &exp(Adj_y) = \begin{bmatrix} \mathbf{t}_\times \mathbf{R} & \mathbf{R} \\ \mathbf{R} & 0 \end{bmatrix}. \end{aligned} \tag{23}$$

Then we can get the transformed noise distribution:

$$y \cdot \tilde{x} \in N(y \cdot x, Adj_y \cdot \sum \cdot Adj_y). \tag{24}$$

VI. Experiment

A. Particularities of UAV

In our experiment, localization of UAV in 3-D space is tested. Quadrotor UAV consists of four rotors which are configured in a cross shape. UAV is equipped with Pixhawk Autopilot which has two advanced processors (32-bit ARM Cortex M4 core with FPU and 32-bit failsafe co-processor). The co-processor has its own power supply even if the other one fails.

B. Particularities of UWB

UWB transceivers used in experiments are P440 modules from Time Domain. The large bandwidth of UWB (from 3.1GHz to 5.3GHz) means that UWB signal is robust to multipath and can provide steady TOA and TDOA measurements. At each time instant, UWB can choose to act as requester or responder. A UWB module can send a ranging request and receive a ranging measurement from another UWB module.

UWB modules need to be calibrated before experiment. Denote the measured distance and the true distance by d and r, respectively. A linear function $d = ar + b$ can be used to calibrate the UWB distance measurement. Parameters a and b can be calculated given a set of samples $(d_i, r_i), (i = 1, 2, ..., n)$. Least square is applied to obtain parameter estimation $\hat{a}$ and $\hat{b}$.

$$\hat{a} = \frac{\sum_{i=1}^{n} (r_i - \bar{r})(d_i - \bar{d})}{\sum_{i=1}^{n} (r_i - \bar{r})}, \tag{25}$$

$$\hat{b} = \bar{r} - \hat{a}\bar{d}, \tag{26}$$

where $\bar{d}$ and $\bar{r}$ are the average distance measurement of d_i and true distance r_i, respectively.

C. Experimental Environment

The UAV tests for 3-D localization were carried out in an area of square $(6m \times 6m \times 3m)$. Four UWB modules are placed in four different fixed positions to serve as anchors. The heights of anchors are also set differently because four non-coplanar points can construct a space. The four anchors are non-coplanar. The UAV is equipped with UWB and IMU sensors.

In this experiment, UAV will send requests to four anchors sequentially to get the distance measurements. The frequency of IMU (100.3 Hz) is about three times larger than that of UWB. The ground truth is provided by a Vicon system which has the accuracy of mm-level. The UAV moved along a circle or a rectangle in our experiments.

D. Comparison with Existing Methods

In the comparison with existing methods, the same devices and same experimental environment are guaranteed. The existing methods are our lab methods presented in [12], [20].

For more than 50 experiments in 3-D space, 5 experiment results are shown in Fig. 2. The comparison with EKF/UKF and nonlinear regression is presented in Table 1. The mean errors of our proposed algorithm in the x and y directions are about 2.3 and 2.2 centimeters and about 7.7 centimeters in the z direction, which are much more than the filter based localization methods which have a mean estimation error of about 6 to 12 centimeters in the x and y directions, and about 25 to 35 centimeters in the z direction.

The box figures of the estimation errors in 3-D space are shown in Fig. 3. For 3-D localization, 75 percent of all estimation errors are within 8 centimeters as seen from Fig. 3. Therefore, our proposed method which integrates IMU with UWB measurements can provide much more localization than the existing filter-based approaches.

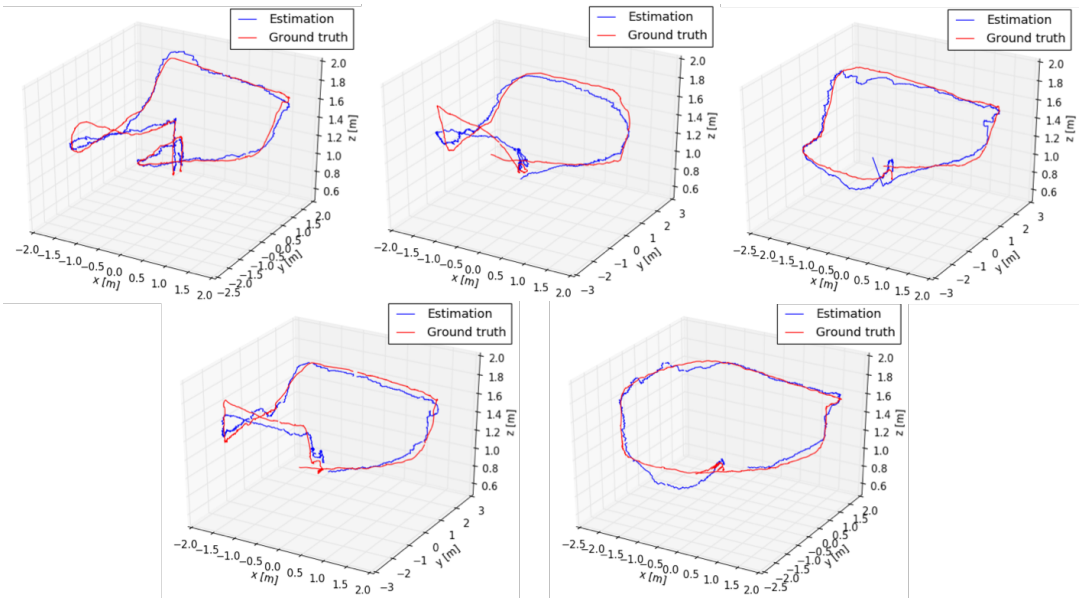

Fig. 2. UAV moved in 3-D space.The red line is Ground truth from Vicon system, and the blue line is the estimation combining UWB and IMU data.

TABLE I

POSITION ESTIMATED 2-NORM ERROR COMPARISON

UAV	UWB + IMU (3-D)	EKF(3-D)	UKF(3-D)	Nonlinear Regression(3-D)
Mean Error of x (m)	0.023	0.114	0.062	0.102
Mean Error of y (m)	0.022	0.123	0.066	0.116
Mean Error of z (m)	0.077	0.353	0.232	0.346

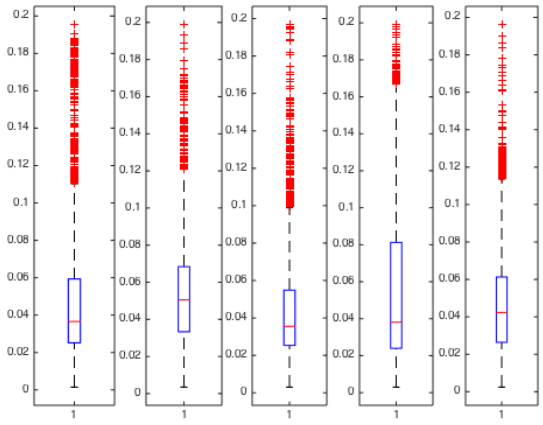

Fig. 3. From box figure, it is shown that 75 percent of all estimation errors are within 8 centimeters.

VII. CONCLUSION

In this paper, an ultra-wideband and IMU aided localization system was proposed based on a graphical optimization approach. The proposed algorithm does not require an kinetic model and can be implemented real-time on a ROS platform. Compared with filter-based localization methods, better accuracy in 3-D space is obtained, especially in the estimation of altitude. The proposed method achieves the graph realization for moving robot under communication limitation of sensors.

REFERENCES

[1] N. A. Alsindi, B. Alavi, and K. Pahlavan. Measurement and Modeling of Ultrawideband TOA-Based Ranging in Indoor Multipath Environments. *IEEE Transactions on Vehicular Technology*, 58(3):1046–1058, Mar. 2009.

[2] T. W. J. M. A. J. D. Ankur Handa. A Benchmark for RGB-D Visual Odometry, 3D Reconstruction and SLAM. *International Conference on Intelligent Robots and Systems*, 2014.

[3] J. Aspnes, T. Eren, D. K. Goldenberg, A. S. Morse, W. Whiteley, Y. R. Yang, B. Anderson, and P. N. Belhumeur. A Theory of Network Localization. *IEEE Transaction on Mobile Computing*, pages 1663–1678, 2006.

[4] A. Benini, A. Mancini, and S. Longhi. An IMU/UWB/Vision-based Extended Kalman Filter for Mini-UAV Localization in Indoor Environment using 802.15.4a Wireless Sensor Network. *Journal of Intelligent & Robotic Systems*, 70:461–476, Aug. 2012.

[5] Z. Chen, H. Zou, H. Jiang, Q. Zhu, Y. Soh, and L. Xie. Fusion of WiFi, Smartphone Sensors and Landmarks Using the Kalman Filter for Indoor Localization. *Sensors*, 15(1):715–732, Jan. 2015.

[6] R. Dalce and A. Van den Bossche. Indoor self-localization in a WSN, based on Time Of Flight: Propositions and demonstrator. *International Conference on Indoor Positioning and Indoor Navigation (IPIN)*, 2013.

[7] D. Dardari, A. Conti, U. Ferner, A. Giorgetti, and M. Z. Win. Ranging With Ultrawide Bandwidth Signals in Multipath Environments. *Proceedings of the IEEE*, 97(2):404–426, Mar. 2009.

[8] C. Di Franco, A. Prorok, N. Atanasov, B. Kempke, P. Dutta, V. Kumar, and G. J. Pappas. Calibration-free network localization using non-line-of-sight ultra-wideband measurements. In *the 16th ACM/IEEE International Conference*, pages 235–246, New York, New York, USA, 2017. ACM Press.

[9] E. Eade. Lie Groups for 2D and 3D Transformations, 2013.

[10] X. Feng, H. snoussi, and Y. Liang. Constrained Extended Kalman Filter for Ultra-Wideband Radio based Individual Navigation. *17th International Conference on Information Fusion*, 2014.

[11] G. E. Garcia, L. S. Muppirisetty, E. M. Schiller, and H. Wymeersch. On the Trade-Off Between Accuracy and Delay in Cooperative UWB Localization: Performance Bounds and Scaling Laws. *IEEE Transactions on Wireless Communications*, 13(8):4574–4585, Mar. 2014.

[12] K. Guo, Z. Qiu, C. Miao, A. H. Zaini, C.-L. Chen, W. Meng, and L. Xie. Ultra-Wideband-Based Localization for Quadcopter Navigation. *Unmanned Systems*, 04(01):23–34, Jan. 2016.

[13] C. Hertzberg. A Framework for Sparse, Non-Linear Least Squares Problems on Manifolds. *Master's thesis*, pages 1–54, 2008.

[14] G. J, J. Blanco, O.-d.-G. A, and F.-M. J A. Mobile Robot Localization based on Ultra-Wide-Band Ranging: A Particle Filter Approach. *Robotics and Autonomous System*, pages 496–507, 2009.

[15] E. Jakob, S. Thomas, and C. Daniel. LSD-SLAM: Large-Scale Direct Monocular SLAM. *European Conference on Computer Vision. Springer, Cham*, pages 834–849, 2014.

[16] R. Kümmerle, G. Grisetti, and H. Strasdat. g2o: A general framework for graph optimization. *IEEE International Conference on Decision and Control*, 2011.

[17] A. Ledergerber, M. Hamer, and R. DAndrea. A Robot Self-Localization System using One-Way Ultra-Wideband Communication. *IEEE/RSJ International Conference on Intelligent Robots and Systems IROS*, pages 3131–3137, Oct. 2015.

[18] X. Longluo, L. Zhiliao, and H. WahTam. Convergence analysis of the Levenberg–Marquardt method. *Optimization Methods and Software*, 22(4):659–678, Aug. 2007.

[19] M. W. Mueller and M. Hamer. Fusing ultra-wideband range measurements with accelerometers and rate gyroscopes for quadrocopter state estimation. *International Conference on Intelligent Robots and Systems*, pages 1730–1736, 2015.

[20] T. M. Nguyen, A. H. Zaini, K. Guo, and L. Xie. An Ultra-Wideband-based Multi-UAV LocalizationSystem in GPS-denied environments. *The International Micro Air Vehicle Conference and Competition*, 2016.

[21] A. Prorok and A. Martinoli. Accurate indoor localization with ultra-wideband using spatial models and collaboration. *The International Journal of Robotics Research*, 33(4):547–568, Apr. 2014.

[22] S. Sen, J. Lee, K.-H. Kim, and P. Congdon. Avoiding Multipath to Revive Inbuilding WiFi Localization. *Proceeding of the th annual international conference on Mobile systems, applications, and services. ACM*, pages 1–14, May 2013.